Apparent Tropospheric Observation of Criegee Intermediate Oligomerization Signatures

R.L. Caravan[1,2,3,*], T.J. Bannan[4], F.A.F. Winiberg[5,6], M.A.H. Khan[7], A.C. Rousso[3,8,†], A.W. Jasper[1], S.D. Worrall[4,††], A. Bacak[4,†††], P. Artaxo[9], J. Brito[10], M. Priestley[4,††††], J.D. Allan[4,11], H. Coe[4,11], Y. Ju[8], D.L. Osborn[3,12], N. Hansen[3], S.J. Klippenstein[1], D.E. Shallcross[7], C.A. Taatjes[3] & C.J. Percival[4,5,*].

[1]Chemical Sciences and Engineering Division, Argonne National Laboratory, Lemont, IL 60439, USA.

[2]NASA Postdoctoral Program Fellow, NASA Jet Propulsion Laboratory, California Institute of Technology, 4800 Oak Grove Drive, Pasadena, CA 91109, USA.

[3]Combustion Research Facility, Mailstop 9055, Sandia National Laboratories, Livermore, CA 94551, USA.

[4]Department of Earth and Environmental Sciences, University of Manchester, Oxford Road, Manchester, M13 9PL, UK.

[5]NASA Jet Propulsion Laboratory, California Institute of Technology, 4800 Oak Grove Drive, Pasadena, CA 91109, USA.

[6]Division of Chemistry and Chemical Engineering, California Institute of Technology, Pasadena, CA 91125, USA.

[7]School of Chemistry, Cantock's Close, University of Bristol, Bristol BS8 1TS, UK.

[8]Department of Mechanical and Aerospace Engineering, Princeton University, Engineering Quadrangle, Olden Street, Princeton, NJ 08544, USA.

[9]Physics Institute, University of São Paulo, Rua do Matão 1371, CEP 05351-015, São Paulo, Brazil.

[10]IMT Nord Europe, Institut Mines-Télécom, Université de Lille, Centre for Energy and Environment, F-59000 Lille, France.

[11]National Centre for Atmospheric Science, University of Manchester, Oxford Road, Manchester, M13 9PL, UK.

[12]Department of Chemical Engineering, University of California, Davis, CA 95616, USA

*Correspondence to: caravarl@anl.gov and carl.j.percival@jpl.nasa.gov

[†]Now at: Computational Engineering Division, Lawrence Livermore National Laboratory, Livermore, CA 95550, USA.

[††]Now at: Aston Institute of Materials Research, Aston University, Birmingham, B4 7ET, UK.

[†††]Now at: Turkish Accelerator & Radiation Laboratory, Ankara University Institute of Accelerator Technologies, Gölbaşi Campus, 06830 Gölbaşi, Ankara, Turkey.

[††††]Now at: IVL Swedish Environmental Research Institute, Aschebergsgatan 44, 411 33, Gothenburg, Sweden.

Abstract:

Criegee intermediates are reactive intermediates that are implicated in transforming the composition of Earth's troposphere and in the formation of secondary organic aerosol, impacting Earth's radiation balance, air quality and human health. Yet, direct identification of their signatures in the field remains elusive. From particulate and gas-phase mass spectrometric measurements in the Amazon rainforest, we identify sequences of masses that are consistent with expected signatures of oligomerization of the CH_2OO Criegee intermediate, a process implicated in ozonolysis-driven aerosol formation. We assess the potential contributions of oligomerization through laboratory ozonolysis experiments, direct kinetic studies of Criegee intermediate reactions, and high-level theoretical calculations. Global atmospheric models built on these kinetics results indicate that Criegee intermediate chemistry may play a larger role in altering the composition of Earth's troposphere than is captured in current atmospheric models, especially in areas of high humidity. However, the models still capture only a relatively small fraction of the observed signatures, suggesting considerable underestimates of Criegee intermediate concentrations and reactivity and/or the dominance of other, presently uncharacterized, oxidation mechanisms. Resolving remaining uncertainties in emission inventories and the effects of atmospheric water vapor on key chemical reactions will be required to definitively assess the role of Criegee intermediate oligomerization reactions.

Main Text:

Alkenes are a major class of chemical species emitted into Earth's troposphere from both anthropogenic and biogenic sources. For example, isoprene (2-methyl-1,3-butadiene) is the most abundant non-methane hydrocarbon in the troposphere globally. It is estimated that isoprene is released by vegetation at ~600 Tg/year [1,2] and is the largest component of biogenic alkenes in

tropical forests[3]. A significant removal process for alkenes in the troposphere (e.g., ~10% of isoprene[4]) is reaction with ozone, which leads to scission of an unsaturated C=C double bond to form two oxygenated reaction products: a stable carbonyl species and a Criegee intermediate (CI),[5] which can be quenched to form stabilized CI (sCI). In the case of isoprene, ozonolysis leads to the formation of three Criegee intermediates: CH_2OO (~58 %), methyl vinyl ketone oxide (~23 %), and methacrolein oxide (~19 %).[4]

Criegee intermediates are important contributors to the oxidizing capacity of the troposphere. Through unimolecular decomposition, they are a major daytime source and the dominant night-time source of the hydroxyl radical (OH) [6-10], the primary tropospheric oxidant that initiates the processing of most atmospheric pollutant species. Following the development of methods to directly study sCI chemistry [11], research has increasingly quantified their role in transforming tropospheric composition. For example, following direct studies of the reaction kinetics of sCIs with SO_2, these reactions are now thought to be a regionally critical pathway for the tropospheric oxidation of SO_2 to SO_3 – a key step in sulphate aerosol formation.[12] Moreover, measurements of have shown that the rate coefficients for sCI reactions with organic acids approach the collision limit.[13-15] Such reactions are significant tropospheric removal pathways for organic acids, especially over regions with large biogenic alkene emissions such as the Amazon rainforest.

Despite their apparent impacts, both sCIs and definitive signatures of sCI-specific reaction products have eluded *in situ* detection in the troposphere. In this work, we examine evidence of signatures of a representative CH_2OO oligomerization reaction sequence in the Amazonian troposphere, which we observe by *in situ* detection in the field. We corroborate the oligomerization mechanism through a combination of direct kinetics measurements, ozonolysis

83 experiments, and high-level theory, and employ the results in an atmospheric model to develop a
84 lower limit prediction for tropospheric concentration of the oligomerization products.

85 The products from sCI + organic acid reactions are promising candidates for detection of sCI
86 signatures in the field due to their characteristic reaction mechanism; rapid insertion of the sCI
87 into the organic acid leads to lower volatility, highly oxygenated reaction products, which are
88 themselves susceptible to reaction with sCIs .[13-16] Field evidence of these sCI oligomerization
89 reactions would be especially compelling because these reaction sequences have been linked to
90 the production of highly oxygenated compounds and secondary organic aerosol (SOA) formation
91 in laboratory experiments [16-19]. SOA is a class of particulate matter (PM) produced from the
92 oxidation of volatile organic compounds (VOCs) and subsequent condensation of the highly
93 oxygenated and low volatility products. [20] SOA constitutes up to 80% of organic particulate
94 mass, which itself accounts for up to 90% of total fine PM mass in the atmosphere [21], yet the
95 pathways leading to SOA formation are not fully understood.

96 Sakamoto *et al.*[16] identified sequences of mass 46 amu (=CH_2O_2) additions in laboratory mass
97 spectrometric investigations of ethene ozonolysis and proposed successive insertion into
98 hydroperoxides by the simplest sCI, CH_2OO; these reactions form a new hydroperoxide as a
99 product, which can react with another CH_2OO molecule. Rousso *et al.* [22] recently identified
100 multiple sequences of CH_2OO additions in laboratory studies of ethene ozonolysis using a jet-
101 stirred reactor (JSR). Recently, various aspects of these sCI oligomerization processes have also
102 been examined theoretically.[23,24]

103 The reaction sequence proposed by Sakamoto *et al.* [16] for highly oxygenated compound and
104 SOA formation may be expected to be most prominent in areas of high alkene emission, such as
105 tropical forests like the Amazon region. Ozonolysis of isoprene and other biogenic alkenes (*e.g.,*

monoterpenes and sesquiterpenes) leads to the formation of the simplest sCI, CH_2OO, as well as unsaturated larger sCIs. In this study, a suite of online measurement techniques was deployed in Central Amazonia. A high-resolution chemical ionization time-of-flight mass spectrometer (TOF-CIMS, masses fitted to < 1ppm) coupled with the filter inlet for gases and aerosol (FIGAERO), hereafter FIGAERO-CIMS, enabled the characterization of oxygenated species in both the gas and particle phases (see SI). We use this technique to identify a series of species that are consistent with multiple, sequential insertions of CH_2OO into formic acid. We have chosen this sequence as a test case because the initial reaction is extremely rapid, its insertion product has been characterized, and the precursor is readily analyzed in the field. Although the TOF-CIMS technique, with its high mass accuracy and sensitivity, is the best available method for detection and identification of these species in the Amazon, the lack of structural information and calibration standards introduces uncertainty into the analysis. Moreover, a multiplicity of oxidation reactions occurs in the Amazon and the complexity of gas- and particle-phase chemical processes in the measurement region inherently limits the certainty of attribution to any particular sequence, especially for larger masses.

In humid regions such as the Amazon, removal of CH_2OO via the reaction with water dimer reduces its lifetime and hence its steady-state concentration; however, other reactions of CH_2OO are also enhanced by water vapor which can increase the effectiveness of CH_2OO as an oxidant [25-28]. The measurements and modelling presented herein, employing advanced theoretical and experimental kinetics, suggest that in areas of high alkene concentrations, Criegee intermediate chemistry persists even in areas of high humidity, and may help drive tropospheric composition changes including contribution to SOA mass. However, the observed concentrations in the putative oxidation sequence remain far larger than the model predictions. Although additional

129 uncertainties in the rate coefficients for Criegee intermediate reactions (including the effect of
130 water vapor) and in the alkene inventory may significantly increase the predicted concentrations
131 for molecules in the oligomerization sequence, the comparison may instead imply that the field
132 concentrations are conditioned by other, presently uncharacterized, oxidation processes.
133

134 **Evidence for tropospheric observation of sCI sequences**

135 Gas-phase FIGAERO-CIMS measurements reveal a series of species with chemical formulae
136 corresponding to the exact masses $HC(O)O(CH_2OO)_nH$ for n=1-6. This result is consistent with
137 multiple, sequential insertions of CH_2OO into formic acid (see SI) as observed in chamber
138 experiments by Sakamoto *et al.* [16] – but not previously observed in the field. Direct calibration
139 for the insertion products is not possible, so the sensitivity must be estimated assuming this
140 reaction to be collision limited. No particle phase calibrations were available, and ROOH species
141 may undergo fragmentation in the the data from the particle phase is qualitative.[29]

142 The correlated diurnal profiles (Figure 1A) of each proposed insertion product from n=2-6
143 support the postulate of cognate origin; correlation with the isoprene, ozone, and formic acid
144 diurnal profiles (see Figure 1B and SI) is direct evidence that even in humid environments,
145 bimolecular reactions of CH_2OO persist in the troposphere (A high background signal on the
146 n=1insertion product mass precludes robust analysis of this species, see SI for the time profile).
147 A gas phase diurnal profile that shows a maximum in the early afternoon and a minimum in the
148 early morning hours is a widely accepted marker of a photochemical oxidation product. [30,31]

149 The relative gas-phase abundances of each sequential insertion product are found to decrease,
150 (see Fig 1 and SI). Successive insertions of CH_2OO into the organic hydroperoxide will result in
151 decreased vapor pressure [32] (see SI), leading to increased partitioning from the gas to the aerosol

phase. This mechanism is further evidenced by the observation of the insertion sequence in the aerosol phase via online high-resolution FIGAERO-CIMS desorption thermogram measurements (see SI). Species with exact masses consistent with *n*=3-5 are observed in the aerosol phase. In the sequential formation pathway, the abundance of products will decrease with increasing *n*.

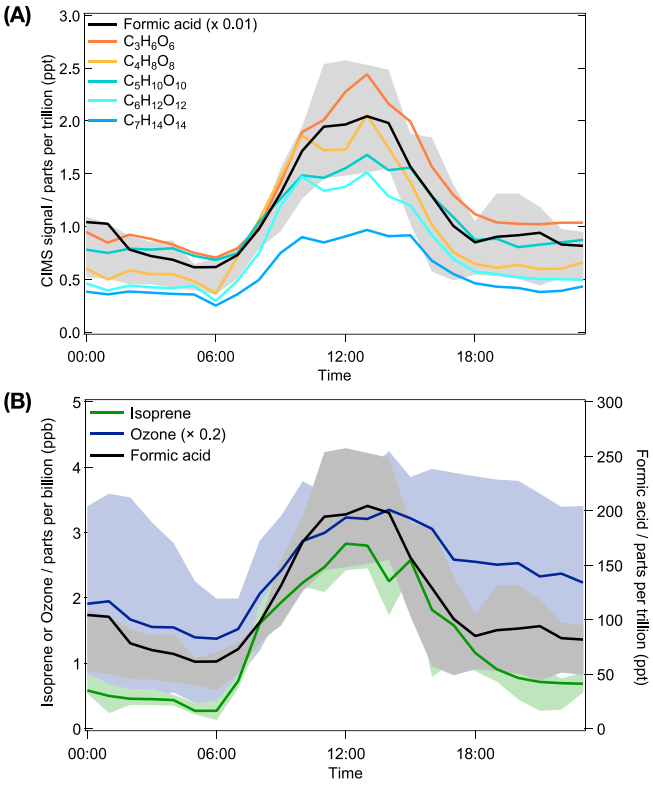

Fig. 1 Evidence of sCI sequences in the Amazon. (A) Gas-phase diurnal profiles of formic acid and insertion sequence products from *n*=2-6 in the gas phase, measured by the gas-phase I^--detection FIGAERO-CIMS experiment. Shaded bar is the 25%- 75% values from the diurnal formic acid concentration. Note that the formic acid signal amplitude is scaled down by a factor of 100 to enable ease of comparison with the *n*=2-6 species. Data presented are the mean profiles throughout the entire campaign. (B) Measured gas phase diurnal profiles of the insertion sequence precursors: isoprene (green), ozone (blue) and formic acid (black). Lines represent the

average measured concentrations; shaded bars are the 25%- 75% values. Data presented are the mean profiles throughout the entire campaign.

After each insertion, only a fraction of the resultant products will undergo further reaction with sCIs due to competing removal pathways (*e.g.,* photolysis, reaction with OH). Thus, for each step of the insertion sequence the concentration of the insertion product will generally decrease. Furthermore, for higher *n*, where the product volatility is sufficiently low, partitioning into the particle phase will compete with further gas-phase reactions, thereby terminating the sequence. The gas-phase and aerosol-phase field observations are consistent with this: in the gas-phase, the insertion product concentration generally decreases with *n* (Figure 1A), and insertion products are observed in the aerosol-phase, for *n*=3-5 (see SI) with decreasing volatility.

These field data provide evidence for the persistence of bimolecular sCI chemistry in the troposphere even in humid environments, and they suggest a potential role for sequential sCI insertion in the formation and growth of highly oxygenated compounds, [33] and SOA mass in the Amazon region. To verify and interpret our field measurements, we have used laboratory experiments to confirm the oligomerization sequence and directly measure representative rate coefficients, and employed accurate theoretical kinetics for experimentally inaccessible reactions to build a detailed picture of the oligomerization process.

Laboratory and theoretical sequence verification

The sequential reactions of CH_2OO were confirmed by laboratory studies of ethene ozonolysis in a JSR (300 K, 700 Torr) coupled to tuneable vacuum ultraviolet radiation (VUV) photoionization (PI) mass spectrometric detection (see SI). At a given mass peak, the PI spectra are used to

chemically identify the species by comparison with known experimental spectra and computed ionization energies (IE). Under the steady-state conditions of the JSR experiment, the sCI is constantly replenished through the reaction of ozone with ethene, enabling subsequent reactions of CH_2OO with primary ozonolysis reaction products.

We detect species at the exact masses consistent with formic acid (m/z = 46.005) and the n=1 and 2 (m/z = 92.011 and m/z = 138.016) CH_2OO insertion products (Figure 2A), in accord with the Amazon field observations, supporting ozonolysis chemistry as the source of the sequence. Comparison of the PI spectra in the present experiment with reference spectra confirms the identity of formic acid and hydroperoxyl methylformate ($CH(O)OCH_2OOH$, HPMF, Figure 2B)[34]. Because no reference PI spectra for the n=2 insertion product exists, the reaction product is identified through high-level theoretical kinetics (discussed later). The calculated IE of the dominant n=2 product (SOZ) determined via theoretical kinetics is consistent with the experimental observations (Figure 2B).

In addition to the formic acid derived sequence, we find evidence of sequential insertion of CH_2OO in the simplest hydroperoxide, hydrogen peroxide (HOOH, H_2O_2), that is formed from the ozonolysis of ethene [22,35], evidence of a general sCI oligomerization mechanism with hydroperoxide functional groups.

Understanding the role that these sequences have in the formation of highly oxygenated, extremely low volatility compounds and SOA in the Amazon requires knowledge of the rate coefficients and products of key sCI + ROOH reactions. Few of these reactions are directly accessible experimentally, including those proposed to result in the observed sequence in the field data. We compare experimental measurements and theoretical predictions for reactions of

CH_2OO with representative ROOH species. We then utilize a closely related theoretical approach for key reactions inferred from the field data.

The reactions of CH_2OO with H_2O_2 and $(CH_3)_3COOH$ were investigated using the photolytic method of Welz *et al.* [11] for the direct production of CH_2OO. Direct kinetics and product measurements were obtained using multiplexed photoionization mass spectrometry (MPIMS), using the same tuneable-VUV detection technique as the JSR experiments (see SI). The MPIMS experiments are time-resolved, thus enabling reactants, intermediates, and products to be simultaneously detected.

Rate coefficients of (2.2 ± 0.9) and $(1.2^{+1.2}_{-0.6}) \times 10^{-13}$ cm^3 s^{-1} were measured for the reactions of CH_2OO with H_2O_2 (at 40 Torr) and $(CH_3)_3COOH$ (at 10 Torr), respectively. Our experimental values for the H_2O_2 reaction compare well to theoretical predictions in the literature (3×10^{-13} cm^3 s^{-1}) [36] and in the present work (2.9×10^{-13} cm^3 s^{-1}, 40 Torr He, 300 K). The present theoretical prediction for the $(CH_3)_3COOH$ reaction (7.4×10^{-13} cm^3 s^{-1}, 10 Torr He, 300 K) is within a factor of three of the experimental upper limit. This agreement supports the reliability of computational methods in more complex analogous reactions in the generalized sequence for which direct experimental studies are not feasible. Reaction products at the exact masses of $CH_2OO + H_2O_2$ (= $C_2H_4O_4$), $CH_2OO + (CH_3)_3COOH$ (= $C_5H_{12}O_4$), and plausible daughter ion species were observed in our direct experimental studies. The growth kinetics of the products and CH_2OO loss kinetics are consistent (Figure 2C), corroborating primary production from CH_2OO reactions.

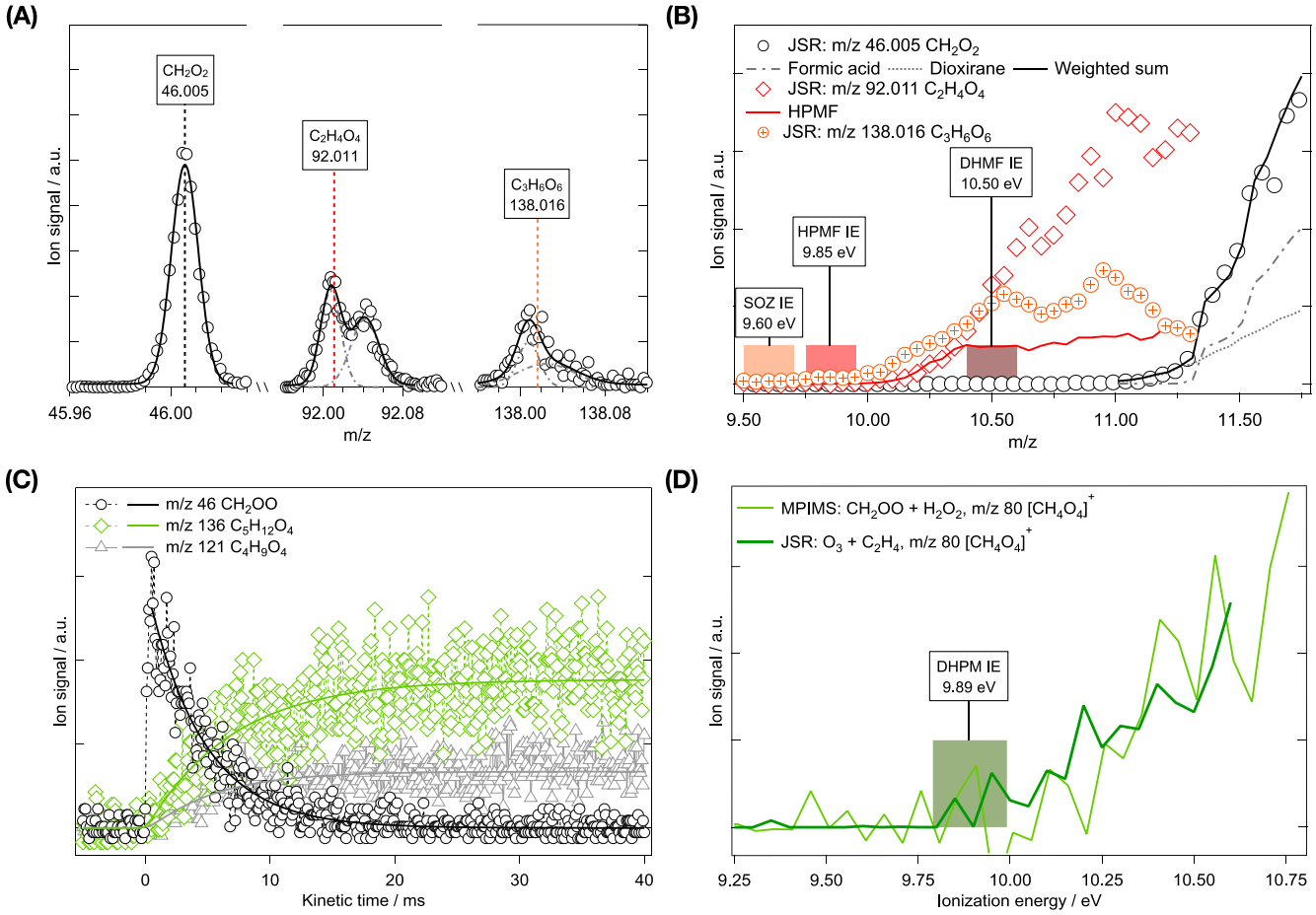

Fig. 2. Laboratory investigations of sCI + ROOH sequences. (A) Mass spectra of the insertion sequence products observed in the JSR O_3 + ethene study. m/z 92 and m/z 138 signal amplitudes are multiplied by factors of 5 and 10, respectively, for visualization. Gaussian multi-peak fits (black solid and grey dot-dash lines) to the data return exact masses consistent with the proposed products along the CH_2OO insertion sequence. (labelled, dashed lines). (B) Measured PI spectra for the m/z 46, 92 and 138 reaction products in the O_3 + ethene JSR study (symbols) compared with calculated IEs (bars) and reference PI spectra [34,35,37] (solid and dashed lines) for species along the sequence of CH_2OO insertion into formic acid (scaled for visualization). A possible contribution from dihydroxymethyl formate (DHMF) as well as HPMF is observed at m/z 92 at higher photoionization energies. (C) Temporal profiles (open symbols) of CH_2OO and

the insertion product ($C_5H_{12}O_4$) and daughter ion, D.I. ($C_4H_9O_4$) from the direct study of CH_2OO + $(CH_3)_3COOH$ using MPIMS (scaled for visualization). Fitting (solid lines) of the kinetic time profiles returns first order rates of 226 ± 12 s^{-1} (m/z 46), 188 ± 44 s^{-1} (m/z 121) and 161 ± 31 s^{-1} (m/z 136), consistent with the direct production of the $C_5H_{12}O_4$ insertion product (plus $C_4H_9O_4^+$ and $C_5H_{12}O_4^+$ D.I.s) from the CH_2OO + $(CH_3)_3COOH$ reaction. (D) Consistent PI spectra of $CH_4O_4^+$ resulting from the reaction of CH_2OO + H_2O_2 (MPIMS, light green line) and O_3 + ethene (JSR, dark green line). The onset of signal is consistent with the calculated IE of dihydroperoxymethane (DHPM, $HOOCH_2OOH$, green bar).

PI spectra of the CH_4O_4 reaction products from the time-resolved, direct experiment of CH_2OO with H_2O_2 and the steady-state, ethene ozonolysis experiment are compared in Figure 2D [22,35]. The similarity of the PI spectra obtained in the direct and ozonolysis studies suggests identical isomeric structure, and theoretical IE calculations identify it as $HOOCH_2OOH$, confirming that both experiments probe the same chemistry. Nowhere previously has the spectroscopy of the reaction products for these oligomerization processes been compared between direct, time-resolved and steady-state ozonolysis experiments. It is the comparison of these spectra that confirm that Criegee intermediates are indeed responsible for the proposed oligomerization products observed in the steady-state experiments. High level quantum chemical calculations to investigate the mechanism of the *n*=2 CH_2OO insertion substantiate a rapid reaction between HPMF and CH_2OO (3.2×10^{-12} cm^3 s^{-1} at 300 K, 1 atm), which primarily generates a reaction product that preserves the -OOH functional group (Figures 3A and 3B). Our predicted rate coefficient for this reaction step lies between two recent density functional theory based theoretical predictions (2.3×10^{-13} and 2.7×10^{-11} cm^3 s^{-1})[23,24] and differ in product predictions. We find that an initial reaction complex between CH_2OO and HPMF yields a hydroperoxyl

secondary ozonide (SOZ) structure, formed from CH_2OO addition over the carbonyl group of HPMF – a mechanism observed in the reactions of CH_2OO with aldehyde and ketone species [38,39]. Under atmospherically pertinent conditions (300 K, 1 atm), master equation calculations predict 62% branching to SOZ and reveal the important role of the pre-reactive van der Waals complex in influencing the product branching fractions (see SI). Calculations reveal that the subsequent reaction of the SOZ with CH_2OO (n=3 in the sequence), proceeds via a submerged transition state to products with a rate coefficient of (2×10^{-13} cm^3 s^{-1}). The dominant product channel (91%) leads to the formation of $SOZCH_2OO$ via CH_2OO insertion into the O-H bond (Figures 3A and C). Crucially, this maintains the -OOH functional group for further, sequential CH_2OO insertions.

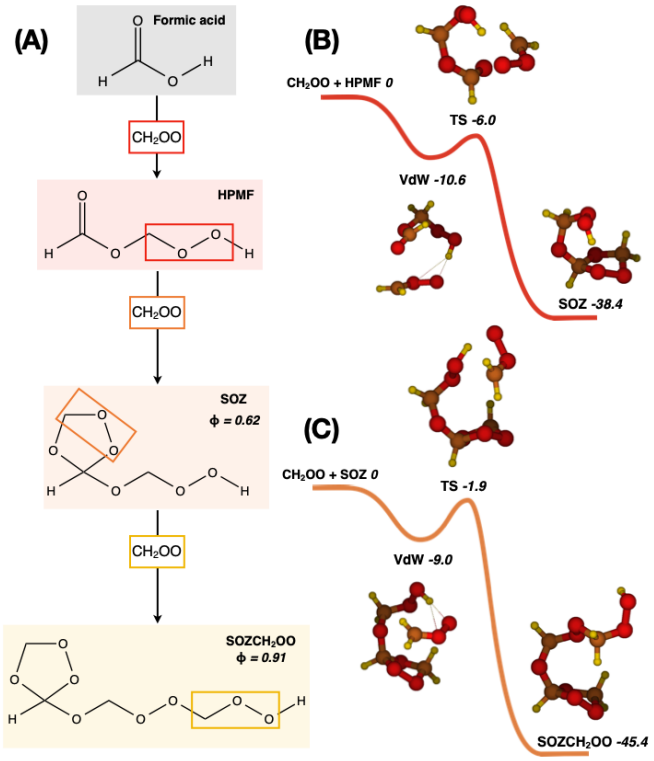

Fig. 3. Theoretical verification of CH_2OO + formic acid sequence. (A) Major pathway for n=1-3 sequential insertions of CH_2OO into formic acid with branching fractions (ϕ) calculated

by high-level theoretical kinetics. (B) Potential energy surface (PES) for the *n=2* insertion reaction of CH_2OO into HPMF (zero-point corrected energies in kcal/mol). (C) PES for the *n*=3 insertion reaction of CH_2OO into SOZ. See SI for further details.

The theoretically determined sequence of CH_2OO insertion into formic acid matches the findings of the JSR laboratory experiments, the field observations in both the gas and aerosol phases, and it is supported by the general reaction mechanism whereby CH_2OO inserts into ROOH, observed in the direct kinetics studies. Coupling the laboratory and theoretical determinations, we have added these CH_2OO-driven reaction sequences to atmospheric chemical models. Comparison of these model results to the field measurements provides a benchmark for the steady-state concentrations of the simplest sCI CH_2OO (denoted $[CH_2OO]_{ss}$) and the initial oligomerization products. For many of the most important atmospheric reactive species, sensitive detection techniques have been developed to measure their steady-state concentrations in the field. However, unambiguous field measurements of sCIs have not yet been realized: recently, atmospheric scientists have made efforts to estimate sCI concentrations using background in laser-induced-fluorescence measurements of OH [40] or by measuring the formation of H_2SO_4 generated by sCI-initiated oxidation of SO_2 [41-44]. But these methods do not unambiguously quantify or speciate sCI. Thus, we are heavily reliant on modelling for our understanding of the tropospheric impacts of sCIs and their chemistry.

Atmospheric implications

Robust modelling of chemistry over the Amazon region is impeded by incomplete model inventories of alkenes. Therefore, to provide a lower limit on the expected oligomerization signal

in the Amazon, we have expanded the alkene inventory in our previous models [45,46] to include sesquiterpenes and more reactive monoterpenes identified by the MEGAN model [,47,48] that will produce CH_2OO and other sCI – bringing our evaluation towards a more accurate representation of Amazon carbon flux. A complete model alkene inventory is also a critical step towards understanding the impacts of sCI chemistry globally. Using the more representative alkene inventory results in modelled $[CH_2OO]_{ss}$ (Figure 4A) [49-51]and total sCI concentrations that are within the bounds of the estimated sCI concentrations reported by Novelli *et al*.[40] (see SI). Using this more representative alkene inventory also increases the reactive loss of modelled OH relative to previous models from 24.4 s^{-1} to 32.6 s^{-1} during dry season and from 20.4 s^{-1} to 23.8 s^{-1} during the wet season in the Amazon area (see Figure 4B for the annual OH loss), whilst not having a significant impact on predicted HO_x, NO_x or SO_x concentrations (See SI). These modelled OH loss rates are more consistent with, but still below, the measured total OH loss (OH reactivity) of up to 60 s^{-1} reported by Nölscher *et al.* [52] and Ferracci *et al.* [53].

This more accurate alkene budget has increased the predicted sCI yield by about a factor of 40 above previous models, but the model still strongly underpredicts the formation of the *n*=2 insertion product (SOZ) compared with that implied by the field measurements (~factor of 2,500, compare Figure 4C and Figure 1A). It is unclear why there is such a significant discrepancy, although there is uncertainty in the measured concentration of insertion products because of the lack of direct calibration. The signatures of sCI chemistry reported herein highlight a need for further development of inventories and kinetic models. There is currently little or no data on the speciated flux measurements of biogenic volatile organic compounds (BVOCs, including monoterpenes, sesquiterpenes) in the Amazon.-[54,55]. Future laboratory and theoretical kinetic investigations on the reactions of more complex, functionalized sCI and ROOH species, that are

especially prominent over the Amazonian troposphere, is an important next step for realizing the impact of this broader class of reactions on tropospheric composition. Detailed kinetic investigations of water-vapor enhament of oligomerization reactions, and incorporation of further insertion steps of sCI into ROOH (e.g., oligomerization) in atmospheric models will clarify the role that ozonolysis-driven chemistry has in SOA formation in the Amazon region and globally.

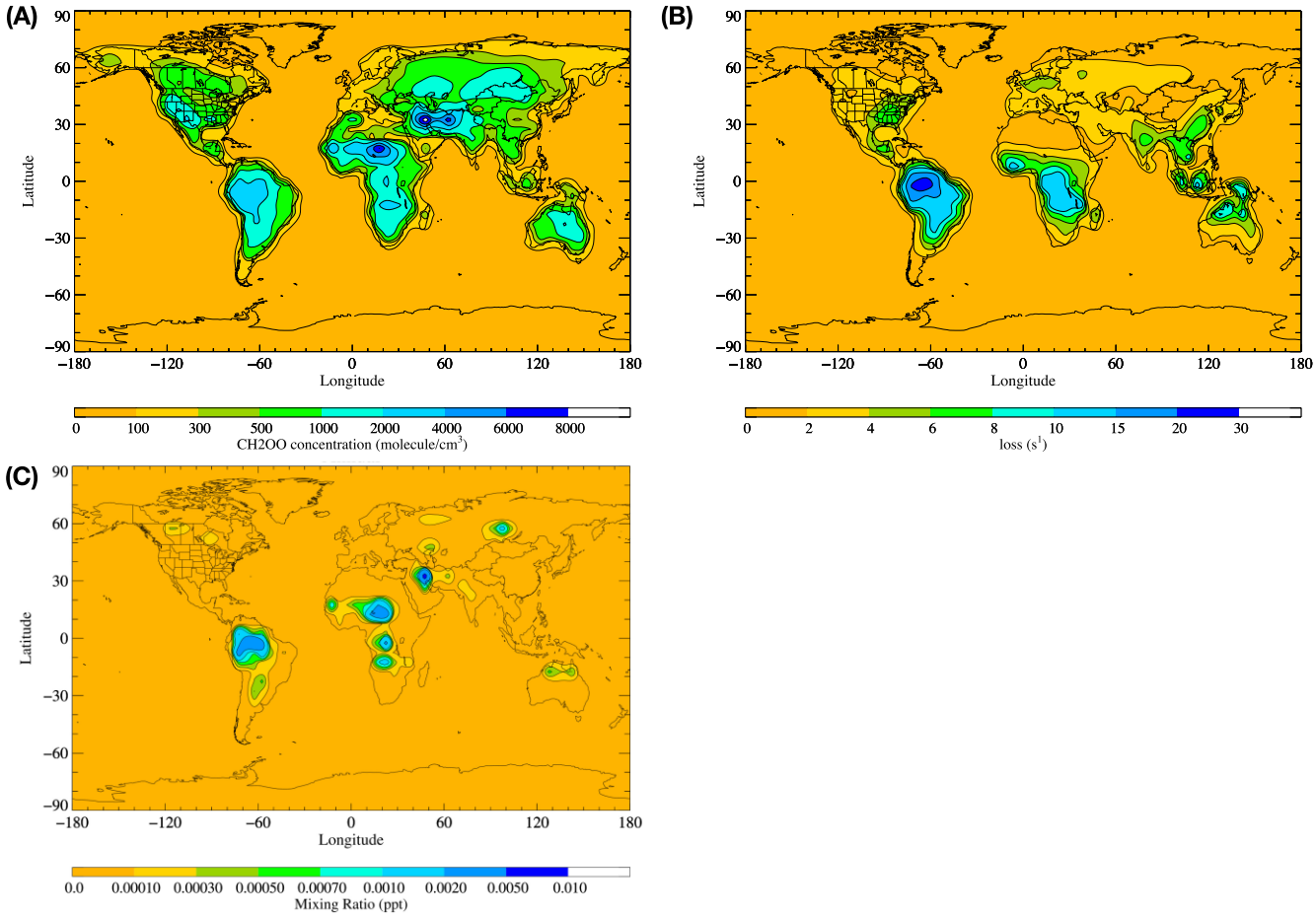

Fig. 4. Modelled impacts of sCI + ROOH oligomerization reactions after including the modified alkene emission inventory. (A) Modelled CH_2OO concentration. (B) Modelled OH

loss rates. (C) Modelled annual mixing ratios of SOZ, resulting from formed from the *n*=2 insertions reaction of CH_2OO into formic acid. The seasonal variation is shown in the SI.

References:

1 Sindelarova, K. *et al.* Global data set of biogenic VOC emissions calculated by the MEGAN model over the last 30 years. *Atmos. Chem. Phys.* **14**, 9317-9341, (2014).

2 Guenther, A. *et al.* Estimates of global terrestrial isoprene emissions using MEGAN (Model of Emissions of Gases and Aerosols from Nature). *Atmos. Chem. Phys.* **6**, 3181-3210, (2006).

3 Kesselmeier, J. *et al.* Atmospheric volatile organic compounds (VOC) at a remote tropical forest site in central Amazonia. *Atmos. Environ.* **34**, 4063-4072, (2000).

4 Nguyen, T. B. *et al.* Atmospheric fates of Criegee intermediates in the ozonolysis of isoprene. *Phys. Chem. Chem. Phys.* **18**, 10241-10254, (2016).

5 Criegee, R. Mechanism of Ozonolysis. *Angew. Chem. Int. Edit.* **14**, 745-752, (1975).

6 Harrison, R. M. *et al.* Measurement and modelling of air pollution and atmospheric chemistry in the U.K. West Midlands conurbation: Overview of the PUMA Consortium project. *Sci. Total Environ.* **360**, 5-25, (2006).

7 Emmerson, K. M. & Carslaw, N. Night-time radical chemistry during the TORCH campaign. *Atmos. Environ.* **43**, 3220-3226, (2009).

8 Emmerson, K. M. *et al.* Free radical modelling studies during the UK TORCH Campaign in Summer 2003. *Atmos. Chem. Phys.* **7**, 167-181, (2007).

9 Khan, M. A. H., Percival, C. J., Caravan, R. L., Taatjes, C. A. & Shallcross, D. E. Criegee intermediates and their impacts on the troposphere. *Environ. Sci.: Process. Impacts* **20**, 437-453, (2018).

10 Lester, M. I. & Klippenstein, S. J. Unimolecular Decay of Criegee Intermediates to OH Radical Products: Prompt and Thermal Decay Processes. *Accounts Chem. Res.* **51**, 978-985, (2018).

11 Welz, O. *et al.* Direct kinetic measurements of Criegee intermediate (CH_2OO) formed by reaction of CH_2I with O_2. *Science* **335**, 204-207, (2012).

12 Percival, C. J. *et al.* Regional and global impacts of Criegee intermediates on atmospheric sulphuric acid concentrations and first steps of aerosol formation. *Faraday Discuss.* **165**, 45-73, (2013).

13 Chhantyal-Pun, R. *et al.* Criegee intermediate reactions with carboxylic acids: a potential source of secondary organic aerosol in the atmosphere. *ACS Earth Space Chem.* **2**, 833-842, (2018).

14 Vereecken, L. The reaction of Criegee intermediates with acids and enols. *Phys. Chem. Chem. Phys.* **19**, 28630-28640, (2017).

15 Welz, O. *et al.* Rate coefficients of C1 and C2 Criegee intermediate reactions with formic and acetic acid near the collision limit: direct kinetics measurements and atmospheric implications. *Angew. Chem. Int. Edit.* **53**, 4547-4550, (2014).

16 Sakamoto, Y., Inomata, S. & Hirokawa, J. Oligomerization reaction of the Criegee intermediate leads to secondary organic aerosol formation in ethylene ozonolysis. *J. Phys. Chem. A* **117**, 12912-12921, (2013).

17 Sadezky, A. *et al.* Oligomer formation during gas-phase ozonolysis of small alkenes and enol ethers: new evidence for the central role of the Criegee Intermediate as oligomer chain unit. *Atmos. Chem. Phys.* **8**, 2667-2699, (2008).

18 Zhao, Y., Wingen, L. M., Perraud, V., Greaves, J. & Finlayson-Pitts, B. J. Role of the reaction of stabilized Criegee intermediates with peroxy radicals in particle formation and growth in air. *Phys. Chem. Chem. Phys.* **17**, 12500-12514, (2015).

19 Chen, L. *et al.* Mechanistic and kinetics investigations of oligomer formation from Criegee intermediate reactions with hydroxyalkyl hydroperoxides. *Atmos. Chem. Phys.* **19**, 4075-4091, (2019).

20 Pandis, S. N. *et al.* Urban particulate matter pollution: a tale of five cities. *Faraday Discuss.* **189**, 277-290, (2016).

21 Carlton, A. G., Wiedinmyer, C. & Kroll, J. H. A review of Secondary Organic Aerosol (SOA) formation from isoprene. *Atmos. Chem. Phys.* **9**, 4987-5005, (2009).

22 Rousso, A., Hansen, N., Jasper, A. & Ju, Y. Identification of the Criegee intermediate reaction network in ethylene ozonolysis: Impact on energy conversion strategies and atmospheric chemistry. *Phys. Chem. Chem. Phys.*, (2019).

23 Chen, L., Huang, Y., Xue, Y., Jia, Z. & Wang, W. Oligomer formation from the gas-phase reactions of Criegee intermediates with hydroperoxide esters: mechanism and kinetics. *Atmos. Chem. Phys.* **22**, 14529-14546, (2022).

24 Chen, M. *et al.* Reaction mechanism and kinetics of Criegee intermediate and hydroperoxymethyl formate. *Journal of Environmental Sciences* **105**, 128-137, (2021).

25 Chao, W., Yin, C., Li, Y.-L., Takahashi, K. & Lin, J. J.-M. Synergy of Water and Ammonia Hydrogen Bonding in a Gas-Phase Reaction. *J. Phys. Chem. A* **123**, 1337-1342, (2019).

26 Chao, W., Yin, C., Takahashi, K. & Lin, J. J.-M. Effects of water vapor on the reaction of CH_2OO with NH_3. *Phys. Chem. Chem. Phys.* **21**, 22589-22597, (2019).

27 Chao, W., Yin, C., Takahashi, K. & Lin, J. J.-M. Hydrogen-Bonding Mediated Reactions of Criegee Intermediates in the Gas Phase: Competition between Bimolecular and Termolecular Reactions and the Catalytic Role of Water. *J. Phys. Chem. A* **123**, 8336-8348, (2019).

28 Lin, Y.-H. *et al.* Criegee Intermediate Reaction with Alcohol Is Enhanced by a Single Water Molecule. *J. Phys. Chem. Lett.* **9**, 7040-7044, (2018).

29 Lopez-Hilfiker, F. D. *et al.* A novel method for online analysis of gas and particle composition: description and evaluation of a Filter Inlet for Gases and AEROsols (FIGAERO). *Atmos. Meas. Tech.* **7**, 983-1001, (2014).

30 Kontkanen, J. *et al.* Simple proxies for estimating the concentrations of monoterpenes and their oxidation products at a boreal forest site. *Atmos. Chem. Phys.* **16**, 13291-13307, (2016).

31 Mohr, C. *et al.* Ambient observations of dimers from terpene oxidation in the gas phase: Implications for new particle formation and growth. *Geophys. Res. Lett.* **44**, 2958-2966, (2017).

32 Kroll, J. H. & Seinfeld, J. H. Chemistry of secondary organic aerosol: formation and evolution of low-volatility organics in the atmosphere. *Atmos. Environ.* **42**, 3593-3624, (2008).

33 Donahue, N. M., Kroll, J. H., Pandis, S. N. & Robinson, A. L. A two-dimensional volatility basis set – Part 2: Diagnostics of organic-aerosol evolution. *Atmos. Chem. Phys.* **12**, 615-634, (2012).

34 Moshammer, K. *et al.* Detection and identification of the keto-hydroperoxide ($HOOCH_2OCHO$) and other intermediates during low-temperature oxidation of dimethyl ether. *J. Phys. Chem. A* **119**, 7361-7374, (2015).

35 Rousso, A. C., Hansen, N., Jasper, A. W. & Ju, Y. Low-temperature oxidation of ethylene by ozone in a jet-stirred reactor. *J. Phys. Chem. A* **122**, 8674-8685, (2018).

36 Vereecken, L., Rickard, A., Newland, M. & Bloss, W. Theoretical study of the reactions of Criegee intermediates with ozone, alkylhydroperoxides, and carbon monoxide. *Phys. Chem. Chem. Phys.* **17**, 23847-23858, (2015).

37 Lin, Z. K., Han, D. L., Li, S. F., Li, Y. Y. & Yuan, T. Synchrotron photoionization mass spectrometry study of intermediates in fuel-rich 1,2-dimethoxyethane flame. *J. Chem. Phys.* **130**, 154306, (2009).

38 Jalan, A., Allen, J. W. & Green, W. H. Chemically activated formation of organic acids in reactions of the Criegee intermediate with aldehydes and ketones. *Phys. Chem. Chem. Phys.* **15**, 16841-16852, (2013).

39 Eskola, A. J. *et al.* Direct kinetics study of CH_2OO + methyl vinyl ketone and CH_2OO + methacrolein reactions and an upper limit determination for CH_2OO + CO reaction. *Phys. Chem. Chem. Phys.* **20**, 19373-19381, (2018).

40 Novelli, A. *et al.* Estimating the atmospheric concentration of Criegee intermediates and their possible interference in a FAGE-LIF instrument. *Atmos. Chem. Phys.* **17**, 7807-7826, (2017).

41 Bonn, B. *et al.* The link between atmospheric radicals and newly formed particles at a spruce forest site in Germany. *Atmos. Chem. Phys.* **14**, 10823-10843, (2014).

42 Boy, M. *et al.* Oxidation of SO_2 by stabilized Criegee intermediate (sCI) radicals as a crucial source for atmospheric sulfuric acid concentrations. *Atmos. Chem. Phys.* **13**, 3865-3879, (2013).

43 Kim, S. *et al.* Potential Role of Stabilized Criegee Radicals in Sulfuric Acid Production in a High Biogenic VOC Environment. *Environ. Sci. Technol.* **49**, 3383-3391, (2015).

44 Sarnela, N. *et al.* Measurement–model comparison of stabilized Criegee intermediate and highly oxygenated molecule production in the CLOUD chamber. *Atmos. Chem. Phys.* **18**, 2363-2380, (2018).

45 Chhantyal-Pun, R. *et al.* Direct Kinetic and Atmospheric Modeling Studies of Criegee Intermediate Reactions with Acetone. *ACS Earth Space Chem.* **3**, 2363-2371, (2019).

46 Chhantyal-Pun, R. *et al.* Impact of Criegee Intermediate Reactions with Peroxy Radicals on Tropospheric Organic Aerosol. *ACS Earth Space Chem.* **4**, 1743-1755, (2020).

47 Jardine, K. J. *et al.* Monoterpene 'thermometer' of tropical forest-atmosphere response to climate warming. *Plant. Cell Environ.* **40**, 441-452, (2017).

48 Guenther, A. B. *et al.* The Model of Emissions of Gases and Aerosols from Nature version 2.1 (MEGAN2.1): an extended and updated framework for modeling biogenic emissions. *Geosci. Model Dev.* **5**, 1471-1492, (2012).

49 Jenkin, M. E., Watson, L. A., Utembe, S. R. & Shallcross, D. E. A Common Representative Intermediates (CRI) mechanism for VOC degradation. Part 1: Gas phase mechanism development. *Atmos. Environ.* **42**, 7185-7195, (2008).

50 Utembe, S. R., Watson, L. A., Shallcross, D. E. & Jenkin, M. E. A Common Representative Intermediates (CRI) mechanism for VOC degradation. Part 3:

Development of a secondary organic aerosol module. *Atmos. Environ.* **43**, 1982-1990, (2009).

51 Watson, L. A., Shallcross, D. E., Utembe, S. R. & Jenkin, M. E. A Common Representative Intermediates (CRI) mechanism for VOC degradation. Part 2: Gas phase mechanism reduction. *Atmos. Environ.* **42**, 7196-7204, (2008).

52 Nölscher, A. C. *et al.* Unexpected seasonality in quantity and composition of Amazon rainforest air reactivity. *Nat. Commun.* **7**, 10383, (2016).

53 Ferracci, V., Heimann, I., Abraham, N. L., Pyle, J. A. & Archibald, A. T. Global modelling of the total OH reactivity: investigations on the "missing" OH sink and its atmospheric implications. *Atmos. Chem. Phys.* **18**, 7109-7129, (2018).

54 Vereecken, L., Novelli, A. & Taraborrelli, D. Unimolecular decay strongly limits the atmospheric impact of Criegee intermediates. *Phys. Chem. Chem. Phys.* **19**, 31599-31612, (2017).

55 Caravan, R. L., Vansco, M. F. & Lester, M. I. Open questions on the reactivity of Criegee intermediates. *Commun. Chem.* **4**, 44, (2021).

Author contributions: Conceptualization: RLC, PA, NH, SJK, DES, CAT, CJP. Methodology: FAFW, MAHK, AWJ, YJ, DLO, NH, SJK, DES, CAT, CJP. Software: FAFW, MAHK, AWJ, DLO, SJK, DES, CAT. Validation: RLC, TJB, FAFW, PA, JB. Formal analysis: RLC, TJB, FAFW, MAHK, AWJ, SDW, NH, SJK. Investigation: RLC, TJB, FAFW, MAHK, ACR, AWJ, MP, NH, SJK, DES, CAT, CJP. Resources: FAFW, ACR, AWJ, MP, DLO, NH, SJK, DES, CAT, CJP. Data curation: RLC, TJB, FAFW, MAHK, ACR, AWJ, SDW, JB, NH, SJK. Writing – original draft: RLC, TJB, FAFW, MAHK, NH, SJK, DES, CAT, CJP. Writing – review and

editing: RLC, TJB, FAFW, MAHK, ACR, AWJ, SDW, AB, PA, JB, MP, JDA, HC, YJ, DLO, NH, SJK, DES, CAT, CJP. Visualization: RLC, TJB, FAFW, MAHK, SJK. Supervision: RLC, JDA, YJ, NH, DES, CAT, CJP. Project administration: RLC, PA, JDA, DLO, NH, SJK, DES, CAT, CJP. Funding acquisition: RLC, AWJ, PA, JDA, HC, YJ, DLO, NH, SJK, DES, CAT, CJP. **Competing interests:** Authors declare no competing interests. **Data Availability:** All data are shown as figures or tables available in the main text or supplementary material. Raw data are available from the corresponding author on reasonable request. **Code Availability:** The codes used for the theoretical kinetics work are available at: https://tcg.cse.anl.gov/papr/ , https://github.com/auto-mech , https://comp.chem.umn.edu/dint/ , https://github.com/Auto-Mech/PIPPy , or are commercially available. The codes used for the atmospheric modelling work are available at https://github.com/chmahk/stochem . **Materials & Correspondence:** Correspondence and requests for materials should be addressed to Carl J. Percival carl.j.percival@jpl.nasa.gov Supplementary information is available for this manuscript.

Acknowledgments: We gratefully acknowledge Kendrew Au, Raybel Almeida and Paul Fugazzi for technical assistance with the MPIMS and JSR experiments. We are grateful to Dr. Arkke Eskola, Prof. Brandon Rotavera, Dr. John Savee, Dr. Oliver Welz, Dr. Ming-Wei Chen, and Dr. Ivan Antonov for early MPIMS attempts. We thank Dr. Samara Carbone for maintaining the ozone, NOx, and ACSM instruments during the field campaign, and the LBA central office at INPA in Manaus for field support. We are grateful to Prof. Richard Evershed, Prof. Andrew Orr-Ewing, Dr. Stephen Pratt, Dr. Stanley Sander, Prof. Linda Young, and Dr. Judit Zádor for useful discussions. **Funding:** This material is based upon work supported by the Division of Chemical Sciences, Geosciences and Biosciences, Office of Basic Energy Sciences (BES), U.S. Department of Energy (USDOE). Sandia National Laboratories is a multimission laboratory

managed and operated by National Technology and Engineering Solutions of Sandia, LLC., a wholly owned subsidiary of Honeywell International, Inc., for USDOE's National Nuclear Security Administration under contract DE-NA0003525. Argonne National Laboratory is supported by the USDOE, Office of Science, BES, Division of Chemical Sciences, Geosciences, and Biosciences under Contract No. DE-AC02-06CH11357. The Advanced Light Source is supported by the Director, Office of Science, USDOE BES under Contract DE- AC02-05CH11231 at Lawrence Berkeley National Laboratory. The contributions of RLC were in part supported by appointments to the NASA Postdoctoral Program at the NASA Jet Propulsion Laboratory, administered by Universities Space Research Association under contract with NASA. This research was carried out in part by the Jet Propulsion Laboratory, California Institute of Technology, under contract with the National Aeronautics and Space Administration (NASA), supported by the Upper Atmosphere Research and Tropospheric Chemistry program. DES and MAHK were supported by NERC (NE/K004905/1), the Primary Science Teaching Trust, and Bristol ChemLabS. The fieldwork was supported by the FAPESP-University of Manchester SPRINT initiative. PA acknowledge funding from FAPESP (Fundação de Amparo à Pesquisa do Estado de São Paulo, 2017/17047-0). This paper describes objective technical results and analysis. Any subjective views or opinions that might be expressed in the paper do not necessarily represent the views of the USDOE or the United States Government.